

REGULAR PAPER

# Molecular hybridization based on (–)-epigallocatechin gallate as a new class of antiglycation agents

Gyeong Han Jeong,<sup>1,†</sup> Seungil Park,<sup>2,†</sup> Seong Bong Kim,<sup>2</sup> Cheorun Jo,<sup>3</sup> and Tae Hoon Kim<sup>1,\*</sup>

<sup>1</sup>Department of Food Science and Biotechnology, Daegu University, Gyeongsan, Republic of Korea; <sup>2</sup>Plasma Technology Research Center, National Fusion Research Institute, Gunsan, Republic of Korea; and <sup>3</sup>Department of Agricultural Biotechnology, Center for Food Bioconvergence, and Research Institute of Agriculture and Life Science, Seoul National University, Seoul, Republic of Korea

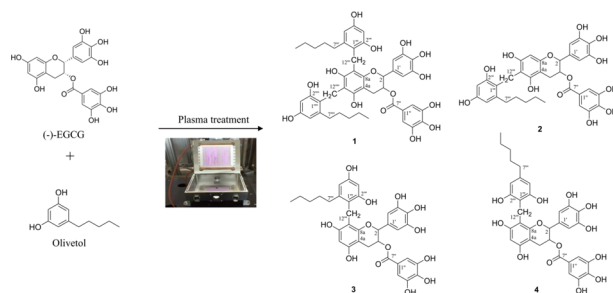
\*Correspondence: Tae Hoon Kim, [skyey7@daegu.ac.kr](mailto:skyey7@daegu.ac.kr)

<sup>†</sup>These authors contributed equally to this work.

## ABSTRACT

(–)-Epigallocatechin gallate (EGCG) and olivetol hybrid molecules 1-4 were conveniently synthesized using dielectric barrier discharge plasma irradiation. The structures of these unprecedented hybrid molecules were determined by interpretation of spectroscopic data. The unusual hybrid 1 showed improved antiglycation potency toward the advanced formation of glycation end products than the original EGCG and olivetol. The novel hybrid 1 is an interesting new class of antiglycation candidate that requires further investigation.

## Graphical Abstract



A new convenient method was established for simple green synthesis of methylene-bridged (–)-epigallocatechin gallate and olivetol hybrid molecules 1-4 using cold plasma apparatus.

**Keywords:** hybrid molecules, (–)-epigallocatechin gallate, olivetol, dielectric barrier discharge plasma, antiglycation

Received: 10 December 2020; Accepted: 19 January 2021

© The Author(s) 2021. Published by Oxford University Press on behalf of Japan Society for Bioscience, Biotechnology, and Agrochemistry. All rights reserved. For permissions, please e-mail: [journals.permissions@oup.com](mailto:journals.permissions@oup.com)

Diabetes mellitus is a common endocrine disease characterized by elevated hyperglycemia. This syndrome is prevalent worldwide and predisposes an individual to chronic complications, including coronary heart disease, nephropathy, and neurodegeneration (Fava 2008; Anselmino 2009). Diabetes-associated metabolic disorder manifests as hyperglycemia, high levels of triacylglycerol (TG), and low levels of high-density lipoprotein (HDL) dyslipidemia. In particular, hyperglycemia resulting from diabetes plays a key role in the pathogenesis of diabetic complications through several mechanisms, such as the increased formation of advanced glycation end products (AGEs), activation of protein kinase C isoform, overexpression of the AGE receptor, excessive oxidative stress, and increased aldose reductase (AR)-related polyol pathway flux in body tissues (Peyroux and Sternberg 2006). The AGEs form in cellular proteins, lipids, nucleic acids, and take complex structures that produce protein fluorescence and cross-linkage. The AGEs and protein glycation are accompanied by increased free radical activity that contributes toward the biomolecular damage in diabetes (Ahmed 2005; Jung et al. 2005). Recent studies have implicated natural and synthetic antioxidants in various diabetic complications in humans (Jung et al. 2005, 2008). Thus, the prevention of AGE formation and oxidative stress is a promising therapeutic target for diabetic complications.

Molecular hybridization is an emerging approach for the advanced strategy of novel chemical entities and structural modifications based on the recognition of pharmacophoric subunits (Viegas-Junior et al. 2007). The chemical hybridization of new prototype drug candidates has attracted considerable attention over the last 2 decades because of their advantageous effects on human health (Proschak, Stark and Merk 2018). Hybrid molecule is created by the combination of structural features of 2 differently active backbones. The development of modified skeletons with enhanced and remarkable properties has been a major focus in the field of medicinal chemistry. In addition, the development of hybrid molecular entities capable of modulating multiple targets is a popular approach for multidrug therapy. Natural products provide an initiating point for new synthetic materials with diverse structures and often have multiple chiral centers, which can be challenging synthetically. Natural bioactive phytochemicals, such as polyphenolic compounds, have attracted recent attention because of their beneficial properties on human health. A previous study reported that the molecular hybridization of natural products with different structural features is a valuable chemical approach for the formation of structurally modified novel entities with improved pharmacological capacities (Suzuki 2010). (–)-Epigallocatechin gallate (EGCG) is the most well-known secondary metabolite of flavan-3-ol found in the leaves of *Camellia sinensis*. This bitter catechin has been studied widely and is believed to have potent biological properties responsible for several beneficial health effects, especially antiglycation capacity (Sampath et al. 2017). On the other hand, (–)-EGCG is unstable under oxidative conditions and has low bioavailability in the human body. Thus, this study examined the influences of its structural hybridization, which is closely correlated with its biological capacity. Several alkylphenol analogs derivatives have promising capacities as a new class of drug candidates in several bioassay systems. Olivetol is found in certain species of lichens and exhibits potent radical scavenging and digestive enzymes inhibitory effects (Taslimi and Culcin 2017, 2018). According to a previous study, EGCG lipophilized with fatty acid is a valuable approach to enhancing the antiglycation activity (Wang et al. 2016). These 2 pharmacologically substantial skeletons were examined to synthesize their molecular hybridization.

Natural products and their semisynthetic derivatives are used extensively in the treatment of several diseases (Kinghorn et al. 2009), but the insufficient amounts of pharmacologically active compounds of natural origins have restricted their application. Moreover, most synthetic procedures for producing pharmacological agents require harsh reactions and long reaction times (Han, Jones and Lei 2015). A recent study suggested nonthermal dielectric barrier discharge (DBD) plasma irradiation as a unique green chemical procedure for the synthesis of structurally novel biologically active compounds with enhanced convenience and yields (Jeong et al. 2017; Jeong, Cho and Kim 2019a). Dielectric barrier discharge (DBD) plasma causes specific chemical modifications due to the generation of abundant oxygen species and reactive nitrogen (Gaunt, Beggs and Georgiou 2006). Recent interest has focused on the synthesis of potential pharmacological agents from major natural products in plant origin. This paper reports the novel structural hybridization of (–)-EGCG and olivetol units adapted by nonthermal DBD plasma irradiation. The present study leads to the unique molecular hybridization of new lipophilized (–)-EGCG analogs with substantially enhanced biological properties based on the formation of AGEs assay compared to the original (–)-EGCG.

## Results and discussion

Cold plasma apparatus irradiation was conducted with a previously described protocol (Jeong et al. 2020). A prepared mixture containing (–)-epigallocatechin gallate and olivetol in methanol was treated directly to DBD plasma for 60 min. The molecular hybridization patterns were monitored with reversed-phase HPLC analysis. Chromatographic separation led to the purification of 4 new methylene-bridged (–)-EGCG-olivetol hybrid molecules 1-4 (Figure 1). The structures of the novel hybrid molecules were established by an interpretation of their spectroscopic data.

Compound 1 was obtained as a white amorphous optically active powder,  $[\alpha]^{25}_D -6.4$  (c 0.1, MeOH). The molecular formula was indicated as  $C_{46}H_{50}O_{15}$  based on the pseudomolecular ion peak at  $m/z$  841.3071  $[M-H]^-$  (calcd for  $C_{46}H_{49}O_{15}$ ) in the negative mode HRFABMS. The UV spectrum exhibited a maximal absorption peak at 225 nm and a broad band approximately 278 nm, which is typical of a flavan-3-ol framework (Cui et al. 1992). The phenolic feature of the hydroxyl groups was evident from a positive ferric chloride test. The  $^1H$  nuclear magnetic resonance (NMR) measurement of compound 1 (Table 1) showed the resonance of 4 sets of *meta*-coupled protons at  $\delta_H$  6.97 (2H, s, H-2'', 6''), 6.70 (2H, s, H-2', 6'), 6.32 (1H, d,  $J = 2.4$  Hz, H-3'''), 6.24 (1H, d,  $J = 2.4$  Hz, H-3'''), 6.17 (1H, d,  $J = 2.4$  Hz, H-5'''), and 6.11 (1H, d,  $J = 2.4$  Hz, H-5'''), indicating the presence of four 1,3,4,5-tetrasubstituted aromatic rings. The spectrum also revealed 2 oxygenated methine protons at  $\delta_H$  5.42 (1H, m, H-3) and 5.00 (1H, br s, H-2), which displayed the characteristic broad singlets at H-2 and H-3 associated with the 2,3-*cis* geometry (Morikawa et al. 2019), and additional 8 methylene protons at  $\delta_H$  2.64-0.91, and 2 methyl groups at  $\delta_H$  .79 (3H, t,  $J = 7.2$  Hz, H-11''') and .60 (3H, t,  $J = 7.2$  Hz, H-11''). With the exception of these resonances, the  $^1H$  NMR spectrum of 1 in the aliphatic area also revealed the resonances of 2 characteristic isolated methylene signals at  $\delta_H$  4.14 (1H, d,  $J = 15.6$  Hz, H-12'''), 3.83 (1H, d,  $J = 15.6$  Hz, H-12'''), 3.80 (1H, d,  $J = 15.6$  Hz, H-12'''), and 3.73 (1H, d,  $J = 15.6$  Hz, H-12'''). Consistent with these  $^1H$  NMR interpretations,  $^{13}C$  NMR and HSQC analyses of 1 further suggested that compound 1 contain 1 EGCG core substituted with 1 olivetol unit. The attachment points of the 2 methylene bridge residues in 1 were established unambiguously through the key HMBC cross-peaks as shown in

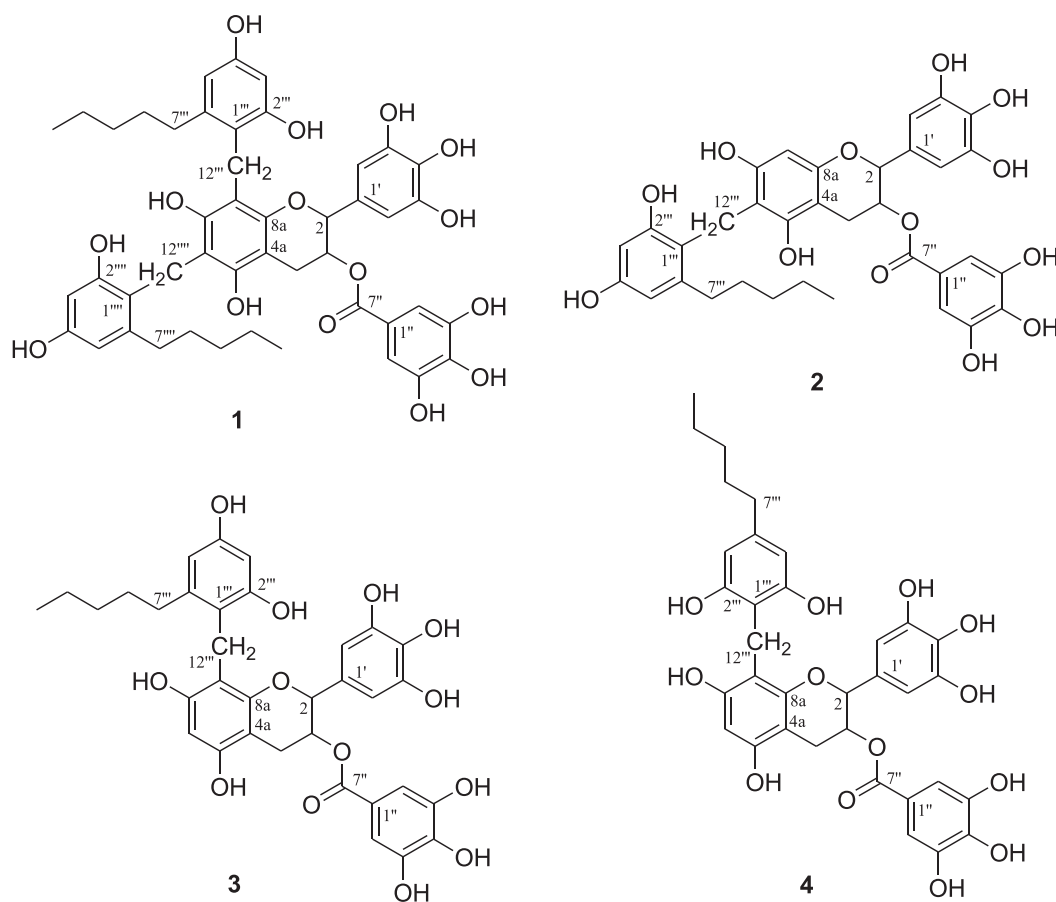


Figure 1. Structures of newly converted hybrid molecules 1-4 induced by plasma irradiation.

Figure 2. The small  $J_{2,3}$  value designated a *cis* stereochemistry between H-2 and H-3 of the flavan 3-ol unit (Morikawa *et al.* 2019). Therefore, the structure of novel hybrid molecule 1 was defined and given the trivial name, olivecachin A.

The negative-ion mode HRFABMS of 2 provided a pseudomolecular ion peak at  $m/z$  649.1915  $[M-H]^-$ , which is consistent with the molecular formula of  $C_{36}H_{33}O_{13}$ . The similar UV and 1D ( $^1H$ - and  $^{13}C$ -) NMR spectroscopic data of these molecules 1 and 2 indicated that 2 was also an EGCG-olivetol hybrid. The  $^1H$  NMR spectrum of 2 (Table 1) observed 3 pairs of *meta*-coupled aromatic signals at  $\delta_H$  6.96 (2H, s, H-2'', 6''), 6.59 (2H, s, H-2', 6'), 6.27 (1H, d,  $J = 2.4$  Hz, H-3'''), and 6.17 (1H, d,  $J = 2.4$  Hz, H-5'''), and 2 diagnostic oxygenated methine protons of the flavan-3-ol moiety at  $\delta_H$  5.35 (1H, m, H-3) and 4.90 (1H, br s, H-2), and 1 methylene signal at  $\delta_H$  2.92 (1H, dd,  $J = 17.4, 4.8$  Hz, H-4) and 2.83 (1H, dd,  $J = 17.4, 1.2$  Hz, H-4), indicating the presence of 1 EGCG and olivetol units. In addition to these characteristic magnetic features, the  $^1H$  and  $^{13}C$  NMR spectra of 2 appeared 1 extra methylene and 1 isolated aromatic singlet functionality at  $\delta_H$  3.83 and 3.73 ( $\delta_C$  18.5) and 6.10 ( $\delta_C$  95.4). The connection point of 1 methylene bridge in the novel hybrid structure was determined unambiguously by the key HMBC cross-peaks between the  $CH_2$ - functionality and aromatic carbons as shown in Figure 2. Therefore, the new structure of 2 could be assigned as olivecachin B as shown in Figure 1.

The  $^1H$  and  $^{13}C$  NMR spectral data of novel hybrids 2 and 3 were closely comparable (Table 1), and the same molecular formula of  $C_{34}H_{34}O_{13}$  was assigned for 2 ( $m/z$  649.1915) and 3 ( $m/z$

649.1927) based on their HRFABMS  $[M-H]^-$ . These 2 compounds were indicated to be olivetol-EGCG hybrids with an olivetol comprising unit substituted in the A-ring of EGCG by a comparison of their 1D NMR data with those of hybrids 2 and 3. Careful interpretation of their 2D NMR (HSQC, HMBC, and NOESY) spectral features resulted in the structural isomer for both 2 and 3. The only difference between 2 and 3 was the linkage points of the olivetol subunits at C-8 or C-6 in the A-ring of the EGCG core. The attached position of olivetol through a methylene bridge at C-8 was clearly indicated by the occurrence of the key HMBC correlations (Figure 2). Thus, compound 3 was structurally assigned as the trivial name olivecachin C.

The negative HRFABMS of 4 exhibited a pseudomolecular ion peak at  $m/z$  649.1927  $[M-H]^-$ , indicating that the molecular formula of  $C_{34}H_{34}O_{13}$  was the same as that of 3. The  $^1H$ ,  $^{13}C$  NMR resonances of 4 were also nearly superimposable to those of 3, except for the presence of a magnetically equivalent 2H-singlet ( $\delta_H$  6.24) instead of the 2 *meta*-coupled aromatic protons in 3. Compound 4 was regarded as the linkage isomer of 3. The location of the methylene bridge in the hybrid molecule was determined by the key HMBC cross-peaks between the  $CH_2$ - functionality and aromatic carbons as shown in Figure 2. Consequently, the structure of 4 was assigned as olivecachin D as shown in Figure 1.

Hybrid compounds are a combination of the structural characteristics of differently active subunits. They are the most popular chemical entities to work upon for emerging modified skeletons with enhanced biological capacities in the field of pharmacology. The synthesis strategy of hybrid natural products

Table 1. <sup>1</sup>H and <sup>13</sup>C NMR shifts of compounds 1-4<sup>a</sup>

Position	1		2		3		4	
	$\delta_{\text{H}}^{\text{b}}$ (J in Hz)	$\delta_{\text{C}}$ , mult.	$\delta_{\text{H}}^{\text{b}}$ (J in Hz)	$\delta_{\text{C}}$ , mult.	$\delta_{\text{H}}^{\text{b}}$ (J in Hz)	$\delta_{\text{C}}$ , mult.	$\delta_{\text{H}}^{\text{b}}$ (J in Hz)	$\delta_{\text{C}}$ , mult.
2	5.00 (br s)	78.1	4.90 (br s)	77.8	5.07 (br s)	78.3	5.17 (br s)	79.5
3	5.42 (m)	69.9	5.35 (m)	70.0	5.45 (m)	69.6	5.44 (m)	69.4
4	2.96 (dd, 17.4, 4.8)	27.2	2.92 (dd, 17.4, 4.8)	26.8	3.02 (dd, 17.4, 4.8)	26.7	2.96 (dd, 17.4, 4.8)	26.6
	2.88 (dd, 17.4, 1.2)		2.83 (dd, 17.4, 1.2)		2.94 (dd, 17.4, 1.2)		2.89 (dd, 17.4, 1.2)	
4a	-	98.9	-	98.9	-	98.7	-	99.4
5	-	153.0	-	154.6	-	155.0	-	154.7
6	-	107.7	-	107.5	5.99 (s)	96.5	6.09 (s)	97.2
7	-	153.2	-	154.8	-	155.3	-	155.5
8	-	106.5	6.10 (s)	95.4	-	106.4	-	105.5
8a	-	151.2	-	154.2	-	153.3	-	152.4
1'	-	130.6	-	130.5	-	130.3	-	129.2
2'	6.70 (s)	106.3	6.59 (s)	106.5	6.71 (s)	106.4	6.76 (s)	108.5
3'	-	146.1	-	146.0	-	146.0	-	145.8
4'	-	132.7	-	132.8	-	132.8	-	133.4
5'	-	146.1	-	146.0	-	146.0	-	145.8
6'	6.70 (s)	106.3	6.59 (s)	106.5	6.71 (s)	106.4	6.76 (s)	108.5
1''	-	121.4	-	121.2	-	121.2	-	121.0
2''	6.97 (s)	109.8	6.96 (s)	109.8	7.02 (s)	109.8	7.08 (s)	110.0
3''	-	145.7	-	145.7	-	145.7	-	146.2
4''	-	138.7	-	138.8	-	138.8	-	139.0
5''	-	145.7	-	145.7	-	145.7	-	146.2
6''	6.97 (s)	109.8	6.96 (s)	109.8	7.02 (s)	109.8	7.08 (s)	110.0
7''	-	166.7	-	166.6	-	166.7	-	166.5
1'''	-	116.4	-	116.4	-	116.7	-	111.6
2'''	-	155.0	-	155.3	-	155.5	-	155.6
3'''	6.24 (d, 2.4)	100.3	6.27 (d, 2.4)	100.3	6.25 (d, 2.4)	100.7	6.24 (s)	106.6
4'''	-	156.7	-	156.7	-	156.5	-	143.2
5'''	6.11 (d, 2.4)	109.5	6.17 (d, 2.4)	107.5	6.15 (d, 2.4)	109.3	6.24 (s)	106.6
6'''	-	145.8	-	145.8	-	145.4	-	155.6
7'''	2.64 (m), 2.34 (m)	33.0	2.62 (m)	33.3	2.72 (m), 2.39 (m)	33.3	2.34 (t, 7.8)	35.9
8'''	1.07 (m)	31.6	1.25 (m)	32.1	1.29 (m)	31.7	1.45 (q, 7.8)	31.4
9'''	0.91 (m)	32.3	1.32 (m)	32.4	1.04 (m)	32.22	1.19 (m)	31.9
10'''	0.93 (m)	23.4	1.20 (m)	23.1	1.01 (m)	23.3	1.23 (m)	22.3
11'''	0.60 (t, 7.2)	14.2	0.80 (t, 7.2)	14.2	0.68 (t, 7.2)	14.1	0.78 (t, 7.2)	14.1
12'''	4.14 (d, 15.6)	18.8	3.83 (d, 15.6)	18.5	4.06 (d, 15.6)	18.6	3.82 (d, 15.6)	16.8
	3.83 (d, 15.6)		3.73 (d, 15.6)		3.76 (d, 15.6)		3.78 (d, 15.6)	
1''''	-	116.3	-		-		-	
2''''	-	154.9	-		-		-	
3''''	6.32 (d, 2.4)	100.4	-		-		-	
4''''	-	156.8	-		-		-	
5''''	6.17 (d, 2.4)	109.7	-		-		-	
6''''	-	145.9	-		-		-	
7''''	2.41 (m)	33.3	-		-		-	
8''''	1.20 (m)	32.2	-		-		-	
9''''	1.15 (m)	31.7	-		-		-	
10''''	1.11 (m)	23.1	-		-		-	
11''''	0.79 (t, 7.2)	13.3	-		-		-	
12''''	3.80 (d, 15.6)	18.6	-		-		-	
	3.73 (d, 15.6)		-		-		-	

<sup>a</sup> <sup>1</sup>H NMR spectra were measured at 600 MHz, and <sup>13</sup>C NMR spectra were measured at 150 MHz. Data obtained in acetone-*d*<sub>6</sub> + D<sub>2</sub>O. Assignments based on HSQC and HMBC spectra.

<sup>b</sup> J values (Hz) are given in parentheses.

has several benefits and can overcome the drug combination accompanying the rapid emergence of drug resistance, potency, solubility, pharmacokinetics, metabolism, and safety (Muregi, Kirira and Ishih 2011). The traditional isolation and characterization of bioactive agents from medicinal plants continues and several naturally occurring phytochemicals have been synthesized into hybrid molecules with remarkably enhanced biolog-

ical capacity using a range of synthetic tools (Perez-Cruz et al. 2013).

Among the representative *Camellia sinensis* catechins, including epicatechin gallate (ECG), epigallocatechin (EGC), epicatechin (EC), EGCG with unstable chemical properties has numerous biological capacities with the potential advantages on human health (Cabrera, Artacho and Giménez 2006). EGCG has poor

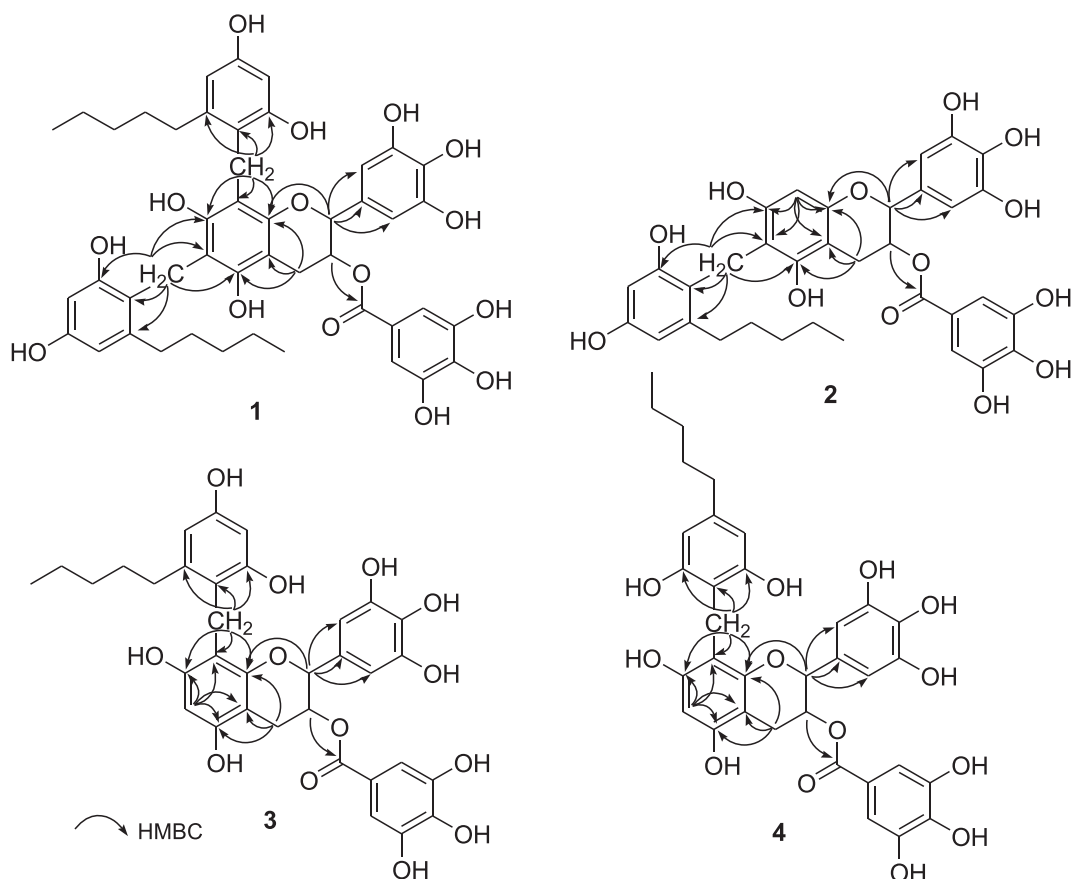


Figure 2. Key HMBC correlations of 1-4.

Table 2. Inhibitory effects on AGEs formation of new hybrids 1-4

Compound	IC <sub>50</sub> value (μM) <sup>a</sup>
Plasma treated (–)-EGCG and olivetol (60 min)	22.9 ± 0.8 <sup>b</sup>
(–)-EGCG	158.1 ± 1.1
Olivetol	>500
1	2.3 ± 0.1
2	7.6 ± 0.4
3	9.8 ± 0.5
4	13.9 ± 0.5
Aminoguanidine <sup>c</sup>	837.2 ± 6.3

<sup>a</sup>Tested compounds were examined in triplicate experiments.

<sup>b</sup>Results are expressed as IC<sub>50</sub> value using μg/mL unit.

<sup>c</sup>Used as a positive control.

bioavailability and bioactivity owing to its relatively hydrophilic nature. To overcome the limitations of EGCG, lipophilized EGCG analogs were synthesized by the esterification of EGCG with different hydrophobic fatty acids (Zhong and Shahidi 2011). Few studies have examined the pharmacological potential of (–)-EGCG-olivetol hybrid using DBD plasma irradiation on antiglycation. Contents of the isolated molecules in the irradiated (–)-EGCG of 30, 60, 90, and 120 min were quantified using the external standard method and the results are shown in Table 3. Five concentrations points ( $n = 5$ ) were used for the preparation of the calibration curve and the calibration curve of pure solutions of the standard compounds was completely linear ( $r^2 > 0.9997$ ). The retention times of newly generated compounds 1 ( $t_R$  19.7 min), 2 ( $t_R$  18.2 min), 3 ( $t_R$  16.8

min), 4 ( $t_R$  19.3 min), olivetol ( $t_R$  20.2 min), and (–)-EGCG ( $t_R$  10.2 min) were detected for 4 plasma-treated samples. Quantitative analysis revealed that the contents of the most potent compound (1) in the treated reactants at 30, 60, 90, and 120 min were  $5.2 \pm 0.3$ ,  $36.3 \pm 1.1$ ,  $43.0 \pm 0.9$ , and  $64.7 \pm 1.3$  mg/g, respectively. As the irradiation dose increased, formation of most active olivocatechin A (1) and new hybrid molecules 2, 3 and 4 increased, reaching maximum values of  $64.7 \pm 1.3$ ,  $172.3 \pm 1.6$ ,  $215.8 \pm 1.8$ , and  $172.3 \pm 1.9$  mg/g upon 120 min treatment, respectively. In contrast, reduction of (–)-EGCG and olivetol contents were observed by DBD plasma irradiation (Table 3). These results suggest that the contents of olivocatechin A (1) and new hybrid molecules 2-4 increased up to 120 min of plasma treatment as the final products from (–)-EGCG and olivetol.

Lipophilized hybrid molecules 1-4 obtained in the present study were evaluated in terms of their inhibitory capacities toward the formation of advanced glycation end products (AGEs) (Table 2) (Vinson and Howard 1996). Among these lipophilized hybrids, olivocatechin A (1) and olivocatechin B (2) exhibited more enhanced inhibitory activities than those of the parent (–)-EGCG and olivetol toward AGEs formation with IC<sub>50</sub> values of  $2.3 \pm 0.1$  and  $7.6 \pm 0.4$  μM, respectively (Table 2). Interestingly, the structurally related hybrids 3 and 4, which have an olivetol moiety on the A-ring at the C-8 position, were found to display relatively weaker inhibitory activity in this bioassay than 1. This suggests that the number and location of hydrophobic olivetol at A-ring for this type of molecule may have positively influenced the inhibition of AGEs formation.

**Table 3.** Content (mg/g) of individual components in the reaction mixture by plasma irradiation times

Compound	$t_R$ (min)	Plasma irradiation time (min)			
		30	60	90	120
EGCG	10.2	534.7 ± 4.4	389.1 ± 2.9	144.7 ± 1.7	57.8 ± 1.0
Olivetol	20.2	215.4 ± 2.1	152.7 ± 1.8	81.1 ± 1.2	Nd
1	19.7	5.2 ± 0.3	36.3 ± 1.1	43.0 ± 0.9	64.7 ± 1.3
2	18.2	22.6 ± .8	28.8 ± 1.0	123.5 ± 1.7	173.2 ± 1.6
3	16.8	46.2 ± 1.0	83.4 ± 0.9	169.8 ± 2.0	215.8 ± 1.8
4	19.3	8.3 ± 0.5	66.1 ± 0.7	136.7 ± 1.6	172.3 ± 1.9

nd: Not detected.

EGCG is the major polyphenolic secondary metabolite in green tea with potent antioxidant capacities that comprise epicatechin and gallic acid comprising units. Based on the chemical structure and molecular weight, phenolic acids and isoflavones are well absorbed. In contrast, catechins and proanthocyanidins are poorly absorbed (Han, Shen and Lou 2007). Structural modification of the attaching lipophilic group to improve its hydrophobicity may be valuable for improving bioavailability and, therefore, bioefficacy. Recent advances have suggested that unstable, reactive oxygen species and free radicals generated by DBD plasma might be conveniently modified to new molecules with enhanced bioefficacy (Jeong, Park and Kim 2019b). The present investigation examined the molecular hybridization and isolation of structurally novel EGCG-olivetol through a methylene bridge that is correlated distinctly with the enhanced antiglycation property.

## Conclusion

The present study found that (–)-EGCG and olivetol is readily hybridized into 4 novel structures 1-4. The new hybrid 1 showed higher antiglycation capacity toward the formation of advanced glycation end products (AGEs) compared to the original EGCG and olivetol. These results will facilitate structure–activity relationship investigations of the antiglycation activities of (–)-EGCG-olivetol connected through methylene bridge compared to other types of hybrid structures. This investigation revealed the convenient hybridization of major naturally occurring secondary metabolites induced by cold plasma and provided a unique approach to the semisynthesis of (–)-EGCG-based hybridization with highly enriched potency for the antiglycation property. A further systematic study into the influences of DBD plasma irradiation on structure hybridization and biological potencies of other natural secondary metabolites is currently underway.

## Experimental

### Chemicals and instruments

(–)-EGCG, olivetol, and aminoguanidine and were purchased from Sigma-Aldrich (St. Louis, MO, USA). All other chemicals used in this study were of analytical grade. UV spectra were recorded on a Hitachi U-2000 spectrophotometer (Hitachi, Tokyo, Japan).  $^1\text{H}$  and  $^{13}\text{C}$  NMR spectra were obtained on a Avance NEO-600 instrument (Bruker, Karlsruhe, Germany) operated at 600 and 150 MHz, respectively. Chemical shifts are given in  $\delta$  (ppm) values relative to those of the solvent acetone- $d_6$  ( $\delta_{\text{H}}$  2.04;  $\delta_{\text{C}}$  29.8) on a tetramethylsilane (TMS) scale. The standard pulse sequences programmed into the instruments were measured

for each 2D measurement. The  $J_{\text{CH}}$  value was set at 8 Hz in the HMBC spectra. FABMS were conducted on a JMS-700 spectrometer (JEOL, Tokyo, Japan). Column chromatography was performed with YMC GEL ODS AQ 120-50S (YMC Co., Kyoto, Japan).

### Sample preparation and new compounds isolation

The plasma exposure device consisted of a process chamber with a DBD apparatus and power supply. The material of the chamber is a Teflon with relatively low chemical reactivity, and the inside of the chamber is  $150 \times 150 \times 275$  (h) mm (Jeong *et al.* 2020). The DBD apparatus is comprised of 4 surface DBD sources. Each source is made of a fused silica plate with a thickness of 0.6 mm and a size of  $100 \times 100$  mm<sup>2</sup> and 2 electrodes of a metal sheet based on nickel–chromium alloy. One electrode consists of  $6 \times 6$  open surface patterns, and each pattern is a rounded square and the size is  $9 \times 9$  mm<sup>2</sup>. The other electrode is no open area. The power supply consists of an arbitrary waveform generator (Tektronix AFG3021C) and a high voltage power amplifier (Trek 5/80). A sinusoidal waveform with a frequency 2.5 kHz and a peak-to-peak voltage of 4 kV was applied between the 2 electrodes during the operation, and surface discharge was generated at the open boundary with 36 patterns in ambient air without any gas supply. The high voltage probe (Tektronix P6015A), 10:1 voltage probe (Tektronix P2100), and 100 nF capacitor were used to measure the dissipated power by plasma. The temperature inside the chamber was measured using a digital hydrometer before and after sample treatment. The dissipated power by plasma is 65 ( $\pm 5\%$ ) W, and the temperature increased from 20 up to 50 °C during the operation. A prepared mixture containing (–)-epigallocatechin gallate (460 mg) and olivetol (180 mg) in methanol (2.5 L) was subjected directly to DBD plasma for 60 min. During that time, the molecular hybridization patterns were observed using reversed-phase HPLC analysis. The exposed methanolic solution treated by DBD plasma was suspended with 10% MeOH (50 mL) and then partitioned with EtOAc ( $3 \times 60$  mL) to afford the dried EtOAc-soluble portion (542.2 mg). A part of the EtOAc extract (470 mg) was directly subjected to column chromatography over a YMC GEL ODS AQ 120-50S column (1.0 cm i.d.  $\times$  43 cm) with aqueous MeOH, to afford pure compounds 1 (2.1 mg,  $t_R$  19.8 min), 2 (5.2 mg,  $t_R$  18.5 min), 3 (9.4 mg,  $t_R$  17.0 min), 4 (2.0 mg,  $t_R$  19.7 min), oolonghomobisflavan A (1.9 mg,  $t_R$  12.5 min), and oolonghomobisflavan B (2.9 mg,  $t_R$  13.8 min). Oolonghomobisflavans A and B were identified by comparison of their spectroscopic data with those of authentic samples and reported data (Hashimoto, Nonaka and Nishioka 1989; Jeong *et al.* 2020). HPLC analysis was conducted on a YMC-Pack ODS A-302 column (4.6 mm i.d.  $\times$  150 mm; 5  $\mu\text{m}$  particle size; YMC Co., Kyoto, Japan), and the gradient solvent system started with 8% MeCN in 0.1% HCOOH/H<sub>2</sub>O (flow rate: 1.0

mL/min; detection: UV 280 nm; temperature: 40 °C), increased to CH<sub>3</sub>CN over 25 min. Newly generated products from original (–)-EGCG and olivetol were identified by comparing their retention times with those of pure (–)-EGCG and olivetol. Quantification of the isolated compounds was carried out by HPLC instruments using the external standard method by constructing standard curves.

### Inhibitions of AGE formation

To evaluate the abilities of EGCG derivatives to inhibit AGEs formation, we used a previously reported method (Vinson and Howard 1996) with minor modification. Briefly, an AGEs reaction solution was prepared by adding 50 mM sodium phosphate buffer (pH 7.4) containing bovine serum albumin (10 mg/mL), and 0.02% sodium azide to inhibit bacterial growth to 0.2 M glucose and 0.2 M fructose. This reaction mixture (950 µL) was then added to samples (50 µL, final concentration 200 µg/mL) dissolved in 5% DMSO. After incubation for 7 days at 37 °C, fluorescence intensities were measured by spectrofluorometry (Infinite F200; Tecan Austria GmbH, Grödig, Austria) using excitation and emission wavelengths of 350 and 450 nm, respectively. The percentage inhibition was calculated from a graphical plot of the data and is expressed as the mean ± SD of triplicate experiments. Aminoguanidine was used as a positive control in the AGE assay.

**Olivecachin A (1):** White amorphous powder,  $[\alpha]_D^{20}$  –6.4 (c .1, MeOH); UV  $\lambda_{max}$  MeOH nm (log  $\epsilon$ ): 225 (2.25), 278 (1.27); CD (MeOH)  $\Delta\epsilon$  (nm): 218 (–23.7), 280 (–4.7); FABMS  $m/z$  841 [M–H]<sup>–</sup>, HRFABMS  $m/z$  841.3071 [M–H]<sup>–</sup> (calcd for C<sub>46</sub>H<sub>49</sub>O<sub>15</sub>, 841.3071); <sup>1</sup>H and <sup>13</sup>C NMR, see Table 1.

**Olivecachin B (2):** White amorphous powder,  $[\alpha]_D^{20}$  –87.4 (c .1, MeOH); UV  $\lambda_{max}$  MeOH nm (log  $\epsilon$ ): 225 (2.28), 278 (1.29); CD (MeOH)  $\Delta\epsilon$  (nm): 215 (–23.8), 278 (–4.6); HRFABMS  $m/z$  649.1915 [M–H]<sup>–</sup> (calcd for C<sub>34</sub>H<sub>33</sub>O<sub>13</sub>, 649.1921); <sup>1</sup>H and <sup>13</sup>C NMR, see Table 1.

**Olivecachin C (3):** White amorphous powder,  $[\alpha]_D^{20}$  –12.6 (c .1, MeOH); UV  $\lambda_{max}$  MeOH nm (log  $\epsilon$ ): 224 (2.26), 275 (1.39); CD (MeOH)  $\Delta\epsilon$  (nm): 214 (–19.3), 278 (–4.9); FABMS  $m/z$  649 [M–H]<sup>–</sup>, HRFABMS  $m/z$  649.1927 [M–H]<sup>–</sup> (calcd for C<sub>34</sub>H<sub>33</sub>O<sub>13</sub>, 649.1921); <sup>1</sup>H and <sup>13</sup>C NMR, see Table 1.

**Olivecachin D (4):** White amorphous powder,  $[\alpha]_D^{20}$  –20.9 (c .1, MeOH); UV  $\lambda_{max}$  MeOH nm (log  $\epsilon$ ): 225 (2.23), 276 (1.23); CD (MeOH)  $\Delta\epsilon$  (nm): 213 (–18.7), 277 (–3.6); FABMS  $m/z$  649 [M–H]<sup>–</sup>, HRFABMS  $m/z$  649.1927 [M–H]<sup>–</sup> (calcd for C<sub>34</sub>H<sub>33</sub>O<sub>13</sub>, 649.1921); <sup>1</sup>H and <sup>13</sup>C NMR, see Table 1.

### Supplemental material

Supplementary material is available at [Bioscience, Biotechnology, and Biochemistry](#) online.

### Author contribution

T.H.K. and C.J. designed the study and prepared the manuscript; S.P., S.B.K., and G.H.J. contributed to the experiments of structure elucidation and biological evaluation and assisted in the design and interpretation of research.

### Funding

This research was supported by R&D Program of ((EN2025–1711124797) through the Korea Institute of Fusion Energy (KFE) funded by the Government funds, Republic of Korea.

### Disclosure statement

No potential conflict of interest was reported by the authors.

### References

- Ahmed N. Advanced glycation endproducts—role in pathology of diabetic complications. *Diabetes Res Clin Pract* 2005;67:3–21.
- Anselmino M. Cardiovascular prevention in type 2 diabetes mellitus patients: the role of oral glucose-lowering agents. *J Diabetes Complications* 2009;23:427–33.
- Cabrera C, Artacho R, Giménez R. Beneficial effects of green tea—a review. *J Am Coll Nutr* 2006;25:79–99.
- Cui CB, Tezuka Y, Kikuchi T et al. Constituents of a fern, *Davallia mariesii* MOORE. II. Identification and <sup>1</sup>H- and <sup>13</sup>C-Nuclear magnetic resonance spectra of procyanidin B-5, epicatechin-(4 $\beta$ →8)-epicatechin-(4 $\beta$ →6)-epicatechin, and epicatechin-(4 $\beta$ →6)-epicatechin-(4 $\beta$ →8)-epicatechin-(4 $\beta$ →6)-epicatechin. *Chem Pharm Bull* 1992;40:889–98.
- Fava S. Role of postprandial hyperglycemia in cardiovascular disease. *Expert Rev Cardiovasc Ther* 2008;6:859–72.
- Gaunt LF, Beggs CB, Georghiou GE. Bactericidal action of the reactive species produced by gas-discharge nonthermal plasma at atmospheric pressure: a review. *IEEE Trans Plasma Sci* 2006;34:1257–69.
- Han J, Jones AX, Lei X. Recent advances in the total synthesis of prenylflavonoid and related Diels–Alder natural products. *Synthesis* 2015;47:1519–33.
- Han X, Shen T, Lou H. Dietary polyphenols and their biological significance. *Int J Mol Sci* 2007;8:950–88.
- Hashimoto F, Nonaka GI, Nishioka I. Tannins and related compounds. XC: 8-C-ascorbyl (–)-epigallocatechin 3-O-gallate and novel dimeric flavan-3-ols, oolonghomobisflavans A and B, from oolong tea. (3). *Chem Pharm Bull* 1989;37:3255–63.
- Jeong GH, Cho JH, Kim SH et al. Plasma-induced dimerization of phloridizin as a new class of anti-adipogenic agents. *Bioorg Med Chem Lett* 2017;27:4889–92.
- Jeong GH, Cho JH, Kim TH. A new approach to procyanidins synthesis with potent anti-adipogenic effects. *Bioorg Med Chem Lett* 2019a;29:2079–84.
- Jeong GH, Kim DH, Jo C et al. Efficient dimerization of (–)-epigallocatechin gallate using nonthermal plasma as potent melanogenesis inhibitors. *J Phys D: Appl Phys* 2020;53:274005.
- Jeong GH, Park EK, Kim TH. Anti-diabetic effects of trans-resveratrol byproducts induced by plasma treatment. *Food Res Int* 2019b;119:119–25.
- Jung HA, Jung YJ, Yoon NY et al. Inhibitory effects of *Nelumbo nucifera* leaves on rat lens aldose reductase, advanced glycation endproducts formation, and oxidative stress. *Food Chem Toxicol* 2008;46:3818–26.
- Jung YS, Joe BY, Cho SJ et al. 2,3-Dimethoxy-5-methyl-1,4-benzoquinones and 2-methyl-1,4-naphthoquinones: glycation inhibitors with lipid peroxidation activity. *Bioorg Med Chem Lett* 2005;15:1125–9.
- Kinghorn AD, De Blanco EJC, Chai HB et al. Discovery of anticancer agents of diverse natural origin. *Pure Appl Chem* 2009;81:1051–63.
- Morikawa H, Okuda K, Kunihiro Y et al. Oligomerization mechanism of tea catechins during tea roasting. *Food Chem* 2019;285:252–9.
- Muregi FW, Kirira PG, Ishih A. Novel rational drug design strategies with potential to revolutionize malaria chemotherapy. *Curr Med Chem* 2011;18:113–43.

- Perez-Cruz F, Vazquez-Rodriguez S, Matos MJ et al. Synthesis and electrochemical and biological studies of novel coumarin-chalcone hybrid compounds. *J Med Chem* 2013;**56**:6136-45.
- Peyroux J, Sternberg M. Advanced glycation endproducts (AGEs): pharmacological inhibition in diabetes. *Pathol Biol* 2006;**54**:405-19.
- Proschak E, Stark H, Merk D. Polypharmacology by design: a medicinal chemist's perspective on multitargeting compounds. *J Med Chem* 2018;**62**:420-44.
- Sampath C, Rashid MR, Sang S et al. Green tea epigallocatechin 3-gallate alleviates hyperglycemia and reduces advanced glycation end products via nrf2 pathway in mice with high fat diet-induced obesity. *Biomed Pharmacother* 2017;**87**:73-81.
- Suzuki K. Lessons from total synthesis of hybrid natural products. *Chem Rec* 2010;**10**:291-307.
- Taslimi P, Gulcin I. Antidiabetic potential: *in vitro* inhibition effects of some natural phenolic compounds on  $\alpha$ -glycosidase and  $\alpha$ -amylase enzymes. *J Biochem Mol Toxicol* 2017;**31**:e21956.
- Taslimi P, Gulcin I. Antioxidant and anticholinergic properties of olivetol. *J Food Biochem* 2018;**42**:e12516.
- Viegas-Junior C, Danuello A, da Silva Bolzani V et al. Molecular hybridization: a useful tool in the design of new drug prototypes. *Curr Med Chem* 2007;**14**:1829-52.
- Vinson JA, Howard TB III. Inhibition of protein glycation and advanced glycation end products by ascorbic acid and other vitamins and nutrients. *J Nutr Biochem* 1996;**7**:659-63.
- Wang M, Zhang X, Zhong YJ et al. Antiglycation activity of lipophilized epigallocatechin gallate (EGCG) derivatives. *Food Chem* 2016;**190**:1022-6.
- Zhong Y, Shahidi F. Lipophilized epigallocatechin gallate (EGCG) derivatives as novel antioxidants. *J Agric Food Chem* 2011;**59**:6526-33.